scientific reports

Check for updates

OPEN

The methodology refinement through the predominant case of the pile-up to estimate the mechanical response by spherical indentation

Habibi Samir[1], Fares Redouane[1], Kiran Batool[2], Sawera Batool[3]✉, Siti Suzilliana Putri Mohamed Isa[4,5], Assmaa Abd-Elmonem[6] & Neissrien Alhubieshi[6]

The purpose of this work is to probe the analytical formulation of the mechanical response R, which is the consequence of determining the connection between charge and depth values. It is possible to acquire the R expression by doing an indentation experiment while the loading process is unfolding. In this particular piece of research, the formulation of R takes into consideration the pile-up mode for an indenter with a spherical structure. The remarkable concordance that exists involving the newly propositioned appearance and the outcome of the experiments has been presented in this academic work. An experimental investigation is being conducted on ductile materials, namely copper and the alloys of copper.

Keywords Spherical indentation, Pile-up, Mechanical response, New expression, Experiments results

Abbreviations

P	Indentations on loading utilized to the indenter
K	A substantial-reliant on fixed called $K-$ factor
K_{SI}	For the sinking-in response, where index SI denotes "sink-in"
K_{PU}	For the pile-up response, wherein subindex PU signifies "pile-up"
h	Indentation depth (the indenter displacement)
Φ, Ψ	Empirical constants
E	Young's modulus
E_R	The reduced Young modulus
H_{IT}	The device stiffness
h	The total indentations depth
h_{cp}	The contact depth
h_{cs}	Denote with sinking-in deformation type
h_{cp}	Denote with pile-up deformation type
h_f	The final indentations depth
A_c	The predicted interaction zone
a	The radius of the circle of interaction at complete loading
Ri	The radius of the indenter
ε	A fixed value equal to 0.75 for spherical indenter
α	A fixed value equal to 1.2
S	The unload interaction hardness at loading P

[1]Industrial Engineering and Sustainable Development Laboratory, Department of Mechanical Engineering, University of Relizane, 48000 Relizane, Algeria. [2]Department of Mathematics, The Women University Multan, Multan 60000, Pakistan. [3]Department of Physics, Benazir Bhutto Shaheed University (BBSU), Peshawar 25000, Pakistan. [4]Institute for Mathematical Research, Universiti Putra Malaysia, Serdang, Selangor Darul Ehsan, Malaysia. [5]Centre of Foundation Studies for Agricultural Science, Universiti Putra Malaysia, Serdang, Selangor Darul Ehsan, Malaysia. [6]Department of Mathematics, College of Science, King Khalid University, Abha, Saudi Arabia. ✉email: saweraktk@hotmail.com

E_s	Young's modulus of indented specimen
ν_s	Poisson's ratio of the indented specimen
E_i	Young's modulus of the indenter
ν_i	Poisson's ratio of indenter

The earliest experiments in material properties where the load and displacement sensing indentation technique has been implemented were performed by Tabor[1]. He reported that the deformed metal indentation was caused by the hardened spherical indenters. Subsequently, a similar experimental apparatus is repeated by using the conical indenters[2]. These studies[1,2] are regarding the effect of when the indenter is unloaded to the shape of the hardness, together with the recovery of the medium elastically. As a result, the accurate relation between the two involved categories has been reported[1], where the first category contained the whole unloading curve and the recovered displacement. Besides, the second category is the contact impression size and the elastic modulus.

The obvious results are the material properties, and the contact area is affected by measuring accurately the total pile-up or sink-in around the indentation. The experimental works regarding the spherical indentation located at the surface deformation, where the correlation between pile-up/sink-in occurrences and the effort-stiffen exponent of the medium[3]. Subsequently, the quantitative function is implemented for the case of the strain- stiffen exponent in the surface deformations across the indentation[4]. The surface profilometry[5] is selected as a method to measure the sink-in and pile-up near the Vickers and spherical indentations in metallic element, and the finite element models (FEM)[6] is used to measure the progress of pile-up near spherical indentation. A wide range of materials with different elastic moduli, yield stress, strain hardening exponent, and friction coefficients were examined. The authors showed parametric plots of the pile-up shape for all considered cases[7–10].

It has been already demonstrated in several research for example[11] that the measurement of indentation load is expressed as:

$$P = Kh^2 \tag{1}$$

where P, h, and K are indicated as indentation load, indentation depth, and K-factor. The indentation load acts towards the indenter, and K also being known as a material-dependent constant. Equation (1) is the alternative option for the classical technique to govern the mechanical properties[12]. Fischer-Cripps[12] did the research by these steps: a) The data from the submicron indentation tests for spherical and Berkovich indenters are collected, b) These data are simulated multiple or single discharge points, c) The simulation technique of an experimental load–displacement response is processed by fixing the input values for modulus of elasticity and hardness.

The authors[11] took the initiative to formulate an analytical expression of the mechanical response K_{SI}, which is presented by including the reduced modulus (sink-in strain case) and the instrumented hardness. However, the authors[13] proposed a different model of this mechanical response K_{PU} as a simple tool for predicting the indentation force and its corresponding penetration depth. Besides, K_{PU} represents the two mechanical characteristics of the pile-up deformation mode. These two models of P/h^2 proposed in sink-in[11] and in pile-up[13] are developed for a pyramidal indent geometry and give two distinct results (see the details in the article[13]). Hence the judicious choice of the predictive function of the behavior of the material is determining and it is dependent on the preliminary choice of the predominant mode of deformation for the precise calculations of the corresponding predictable interaction area either by the method[14] or[15].

However, Fischer-Cripps[12] has proved that the elasto-plastic properties and the indenter tip geometry influence the K-factor value. After some research works for some materials such as fused silica and steel, Fischer-Cripps[12] introduced the innovated K-factor for spherical indenter as below:

$$K_{SI} = E_R \left(\frac{a}{2R\sqrt{\pi}} \sqrt{\frac{E_R}{HIT}} + \varepsilon \sqrt{\frac{\pi}{4}} \sqrt{\frac{HIT}{E_R}} \right)^{-2} \tag{2}$$

where the HIT, E_R, and index SI denote the instrumented rigidity, reduced Young's formula, and "Sink-In". In addition, for the conical and spherical indenters, $\in = 0.75$.

The lowered modulus E_R is expressed as:

$$\frac{1}{E_R} = \frac{1-\nu_i^2}{E_i} + \frac{1-\nu_m^2}{E_m} \tag{3}$$

where the Poisson's ratio of the indenter and the Poisson's ratio of the material is denoted by (E_i, ν_i) and (E_m , ν_m), respectively.

The sink-in distortion case near the indentation is successfully solved by using Eq. 2, where this equation is independent of the deformation mode. However, this equation cannot be used for pile-up since it involves hardness property. Spherical indents are generally preferred in the circumstance of soft resources. If the applied force is low, they mainly produce elastic deformations. At higher indentation loads, the strains produced are more of the elastoplastic type, allowing the study of plasticity or strain hardening in the elastic–plastic transition. Therefore, this paper aims to develop the mechanical response in the situation of pile-up distortion mode near the spherical indenter geometry, more precisely K_{PU}. It involves Young's modulus and the instrumented rigidity.

Next, the model presented in this study is then employed to the copper and its alloys describing the mode of pile-up deformation, namely brass, bronze, etc.

Materials and experimental methods

Three specimens were selected, such as copper, bronze, and brass, with the specification 99% purity, SAE 660, and 63/37 C27200, respectively. Their chemical symbols are expressed as Cu99, SAE660, and C27200 respectively. This paper aims to verify the model, together with its methodology instead of studying the mechanical features of these specimens. These specimens are used in experiments of instrumented indentation, and they have been prepared with the proper steps to control the surface roughness and the outline of straining hardening in line for improvement. The next step is SiC papers and a finishing polishing is used to ground the specimens. The SiC papers are in diverse grit sizes, whereas the finishing polishing used the diamond pastes series with the grit size = 1 mm.

The microhardness Tester CSM 2–107 functions to run the instrumented indentation tests. This tester has a spherical indenter of radius equal to 0,1mm. For a diamond indenter, $E_i = 1140GPa$ and $\nu_i = 0.07$ [16]. The scale of the load (namely by R) on the instrument is $0.1 < R < 30N$. Regarding CSM Instruments Group, the load resolution and the depth resolution are 100 mN and 0.3 nm, separately. Table 1 shows the loading scale and the amount of applicable indentation tests from 2011 until 2015.

From Table 1, about 20 indentation tests were run for the range of indentation loads from 0.02 to 10 N. The rates of the loading and unloading are 2 times by maximum applied load value[17], and these rates are in mN/min . The dwell time is 15 s for the indentation test ASTM E92 and E384-10e2.

Background theory

The determination technique for HIT and E in indentation[14] is widely applied. However, this technique is invalid for pile-up cases in deformation mode[15]. This is the valid reason; the HIT and E calculations are presented in two separate cases.

Therefore, HIT is represented as:

$$HIT = \frac{P}{A_c} \tag{4}$$

wherein P and A_c are the applied load and the predicted contact zone, separately. Next, A_c is formulated as

$$A_c = \pi a^2 \tag{5}$$

where a is the radius of the interaction area and it has its specific formula:

$$a = (2R_i h_c)^{0.5} \tag{6}$$

where R_i is the indenter radius. As a result, A_c can be expressed as:

$$A_c = \pi(2R_i h_c - h_c^2) \cong 2\pi R_i h_c \tag{7}$$

where $h_c < R_i$.

The HIT involving the spherical indentation is as follows:

$$H = \frac{P}{2\pi R_i h_c} \tag{8}$$

The E_R formula offered by Ref. [14] which can be applied to any indenter geometry is as below:

$$E_R = \frac{S}{2}\sqrt{\frac{p}{A_C}} \tag{9}$$

whenever the concentrated modulus is linked to the elastoplastic possessions of the indenter and of the verified substantial as declared in (3). In addition, S is the contact stiffness, which is presented as a differentiation of the indentation load P towards h when h is maximum:

Date month/year	Reference	Poisson's ratio n	Young's modulus $E\ (GPa)$	Loads range	N_b tests
07/2011	SAE660	0.30	≅ 100	0.2–10 N	23
07/2011	Cu99	0.28	≅ 120	0.2–20 N	24
01/2015	C27200	0.36	≅ 110	0.02–10 N	23

Table 1. Materials and indentation conditions with the loads' range and valid tests.

$$S = \frac{dP}{dh}\Big]_{h=h_m} \tag{10}$$

Subsequently, P can be calculated from the gradient of h (instantaneous h and final h_f):

$$P = B(h - h_f)^m \tag{11}$$

wherein the values of B, m, and h_f are fixed from a stage via stage best-fit investigation. Now actual situation, the depression values around 40–98% of the maximum load are chosen.

The $P - h^2$ model aimed at the pile-up deformation style

The deformation mode influences the contact depth h_c. Therefore, the model for the sink-in case is proposed[14]. However, the proposed technique[15] is inappropriate for the pile-up case whether their method is significantly employed in the deformation mode. For the pile-up case, Refs.[15,18–20] introduced the relationship of $h_c > h_m$.

However, this relationship is opposite to the sink-in case[10]. As a result, the connection depth measured by Refs.[15,18–20] is higher than Oliver and Pharr[14] where this comparison is obtained from an indentation test (Fig. 1). This test is conducted with the same applied load and indenter depth. Therefore, the inaccurate estimation for the instrumented hardness and Young's modulus (too high or too low) cannot be avoided because this step depends on the selected deformation mode and the contact depth is also difficult to estimate accurately. In the same indentation test, these two techniques cannot converge. Hence, the deformation mode must be declared earlier. The contact depth, together with the index cp (pile-up deformation mode) can be computed from Eq. 12 since it determines the interaction area regarding the deformation type.

$$h_{cp} = \alpha\left(h_m - \frac{P}{S}\right) \tag{12}$$

where $\alpha = 1.2$. In the subsequent part, the $R-$ factor can be derived for pile-up deformation type. This derivation is obtained constructed on the concept of the interaction depth calculation and the mechanical properties.

Consequently, starting from Eq. (13) for pile-up, it is obtained:

$$\text{For pile} - \text{up} : h_m = \frac{1}{\alpha}.h_{cp} + \frac{P}{S} \tag{13}$$

Next, the P/S ratio is:

$$\frac{P}{S} = \frac{\sqrt{P\pi H}}{2E_R} \tag{14}$$

The hardness H is used to express h_{cp}:

$$h_{cp} = \frac{P}{2\pi R_i H} \tag{15}$$

Equations (14) and (15) are substituted into Eq. (13), and the result is:

$$h_m = \frac{1}{\alpha}.\left(\frac{P}{2\pi R_i H}\right) + \left(\frac{\sqrt{P\pi H}}{2E_R}\right) \tag{16}$$

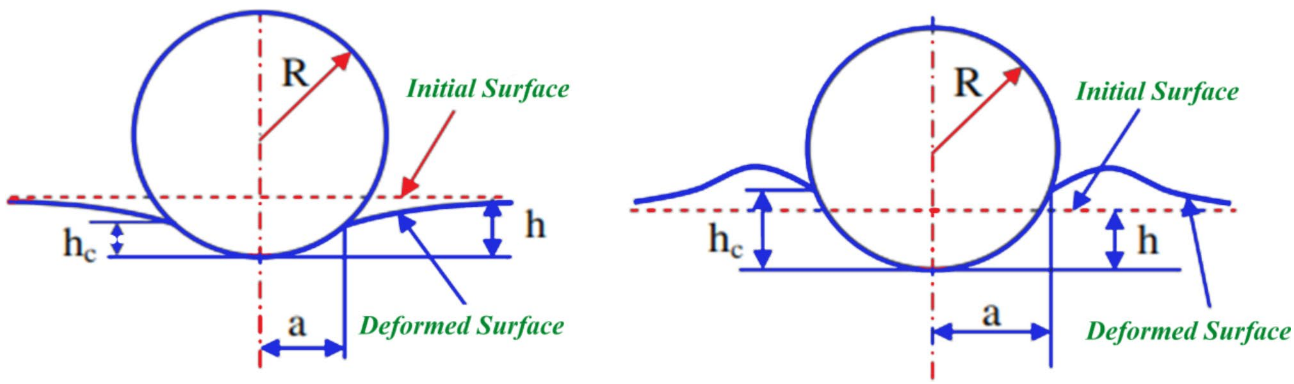

Fig. 1. The representation of material around spherical indents for the cases of (**a**) sinking in and (**b**) piling up[14].

Models	Deformation mode	Indenter geometry	Constant factors	
			ϕ	Ψ
Fischer-Cripps (see Eq. (2) [12])	Sink-in	Spherical	0.015	0.664
This effort (see Eq. (18))	Pile-up	Spherical	0.012	0.886

Table 2. The constant factors of ϕ and Ψ for specific models and deformation mode.

Designation	Classical $E\,(GPa)$	h_f/h_m	Sink-in mode		Pile-up mode	
			$HIT_{SI}(GPa)$	$E_{SI}{}^{(*)}\,(GPa)$	$HIT_{PU}(GPa)$	$E_{PU}{}^{(*)}\,(GPa)$
SAE660	≅100	0.87	1.26	185	1.10	160
Cu99	≅120	0.88	0.99	115	0.89	108
C27200	≅100	0.89	0.93	79	0.86	76

Table 3. The mechanical attributes were estimated using Oliver and Pharr's[14] methodology under the assumption of sinking-in and Refs.[15,18–20] approach under the assumption of pile-up, with the h_f/h_m ratio indicating the distortion phase being h_f/h_m < 0.83 aimed at sinking-in and $h_f/h_m > 0.83$ for pile-up[21,22]. *Note that E_{SI} and E_{PU} are Young's modulus of the confirmed resources and not the condensed modulus.

Subsequently, the relation between indentation depth and displacement for the pile-up deformation mode is derived:

$$P_m = \left[\frac{a}{2.\alpha.R_i.\sqrt{\pi}}\frac{1}{\sqrt{H}} + \frac{\sqrt{\pi}}{2}.\frac{\sqrt{HIT}}{E_R}\right]^{-2}.(h_m + h_0)^2 \tag{17}$$

The contacting depth defined by Refs.[15,18–20] as the greatest degree of indentation in Eq. (14) Therefore, the extreme depth is the supreme load, or the depth measured by the position of indentation for a certain load and indicated by h. For the instance of the entire loading curve, the notion h_m can be replaced by h. As a result, the K factor for the pile-up distortion style is stated similarly as Eq. (2) presented below:

$$R_{PU} = E_R\left(\frac{a}{2.\alpha.R_i.\sqrt{\pi}}\sqrt{\frac{E_R}{HIT}} + \frac{\sqrt{\pi}}{2}\sqrt{\frac{HIT}{E_R}}\right)^{-2} \tag{18}$$

By the analogy of the Fischer-Cripps expression[12] and the expression proposed in this work, to the reference model proposed by Hainsworth et al.[11], the coefficients ϕ and Ψ of Eq. (2) and Eq. (18) differ according to the two modes of deformation according to the Table 2.

To validate the $K-$factor, it is discussing below the influence of indenter spherical geometry on the HIT, E_R and $K-$factor. Next, the calculated $K-$factor from this article is compared to the experimental $K-$factor. To verify the pertinence, the models are set to be independent of the deformation mode.

Results and discussion

The choice is made on seven curves of loading and unloading by spherical indentation by way of example based on twenty-four curves in total for better visibility of the tendencies of the curves.

The experimental function P/h^2 is expressed as a function of the two key parameters of the mechanical characterization HIT and EIT. The use of the methods recommended by[14] and [15] concerning the sink-in and the pile-up, correspondingly. Give different results aimed at instrumented hardness and modulus of elasticity between these two modes of deformation. The hf/hm criterion[21,22] predicts that the predominant strain mode is the pile-up concerning these three reference materials taken as examples to validate the model proposed in this article. As the results displayed in the following comparison Table 3 clearly shows:

The constituents of the K_{SI} and K_{PU} responses, namely HIT and E_R, vary from one model to another. Hence, we examine the evolution of these responses as a function of their primitive function P/h^2. Linear regressions make it possible to show the two mechanical responses K_{SI} and K_{PU} generated by the experimental function P/h^2 resulting from spherical indentation, as shown in Fig. 2:

Also, this regression by transitivity between (K_{SI}, P/h^2) and (P/h^2, K_{PU}) highlights the proportionality relationship between Ksi and Kpu as indicated by the following Eq. (19):

$$R_p = 0.9796 * Rs + 4.3228 avec R^2 = 1 \tag{19}$$

Hence a difference of the order of 2.20% is estimated between the mechanical reactions planned by the analytical expressions (2) and (18) proposed by[12] and the present work, respectively. The collocation of the characteristic points of the two functions K_{SI} and K_{PU} show their excellent factorial correlations with the experimental

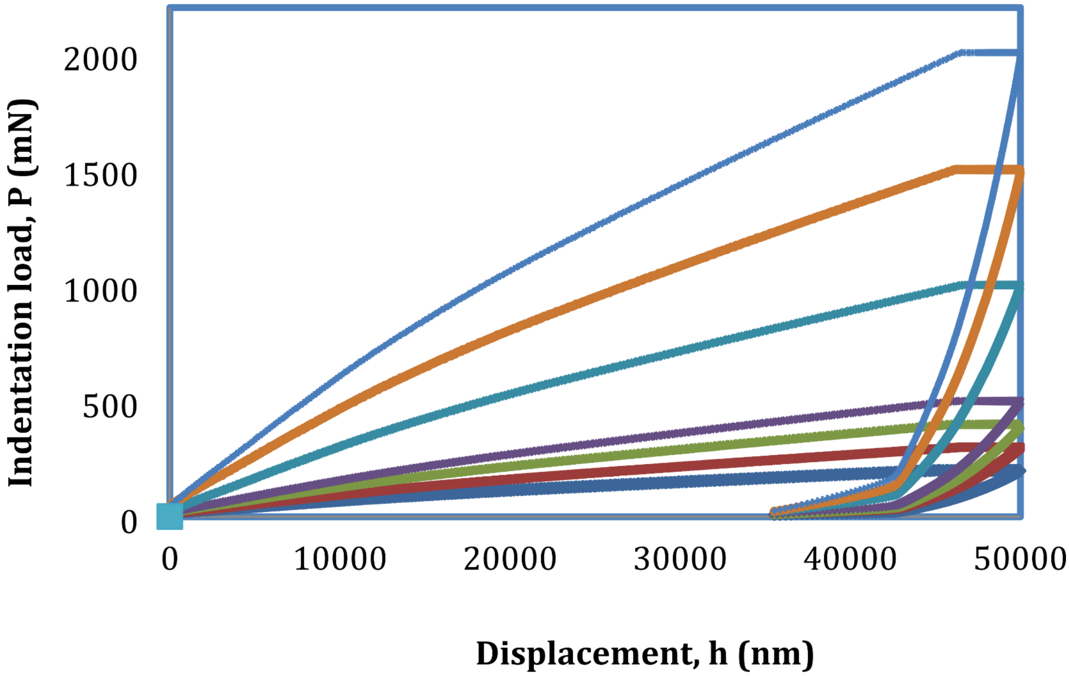

Fig. 2. The response of the spherical indentation $P - h$ of copper obtained from experimental tests at a loading range.

function, P/h^2. However, the difference between the two linear regressions is visible and tends to influence the results between the two chosen expressions. This difference is considered insignificant at the macro scale, but it is likely to affect their precision at the micron scale and even more at the nanoscale. Hence the choice of an expression corresponding to a designated mode of deformation is decisive for the reliability of the expected precision of the mechanical properties.

The alternative use of one expression to the detriment of another out of ignorance or ignorance implies errors in the results. Hence, the concern is to assess this gap to assess the impact of one mode on the other. Figure 2 indicates the amplitude of the difference between the findings of the two analytic formulas used for the computation of the mechanical response by spherical indentation in sink-in (Eq. (2)) and pile-up (Eq. (18) modes), respectively.

Each characteristic column of the histogram (see Fig. 3) denotes an indentation test. The thirteen tests illustrated in Fig. 3 are representative of the 24 tests for a clearer presentation of the amplitude columns resulting from the estimated differences between the responses K_{SI} and K_{PU} respectively. There is indeed a difference between the trends of the K_{SI} and K_{PU} curves which is shown in Fig. 3. This difference is estimated for each indentation test with previously defined loading (see Fig. 3). This difference varies from test to test. Since the responses K_{SI} and K_{PU} are made up of E_{RS}, E_{RP}, HIT_S, HIT_P, ε, α, and without forgetting the contact radius ac. recognizing that a function of contact depth is used to denote mechanical characteristics including hardness, Young's modulus, and contact radius. This depth is a constituent factor of the mechanical footprint. This challenges us to make the judicious choice of the equation corresponding to the mode of deformation in sinking-in or pile-up. And whose role of ε and/or α is preponderant in the calculation of mechanical properties such as HIT and E_R. Substituting one coefficient for the other (ε or α) surely generates an appreciable difference in the findings of the mechanically responses R_{SI} and R_{PU} as shown in Fig. 3. The comparisons of the outcomes of the analytic formulas proposed by Fischer-Cripps[12] and this work with the results relating to the experimental expression P/h^2 are shown in histogram 5, for the three materials examined, as follows:

It is evident by the comparative histogram 5 between the three expressions of calculation that the expression of the pile-up proposed in this article and that of the direct calculation, P/h^2 register an excellent correlation which tends to confuse shapes of their column's characteristics for copper and its two alloys. However, the analytical expression relating to the sink-in[12] records a small variable deviation from the other two during the various indentation tests. Even if this deviation evaluated in histogram 5 is small (weak) it reflects that the analytic representations purported in the current examination (see Eq. 18) for the pile-up is more adapted to these solid elastoplastic materials having deformations of the type of pile-up.

The analysis of the loading cycle of the characteristic curves relating to the different loadings (see Fig. 4), shows a difference observed between the two mechanical responses in sink-in, K_{SI}, and in the pile-up, K_{PU}, respectively (see Figs. 3 and 5). Estimated in percentages at 2.7%, 2.2%, and 2.6% for materials; SAE660, Cu99, and C27200, respectively (see Table 4). We also observe a better correlation between the ratios derived from the expressions of K_{PU} and K_{EXP} compared to that of K_{SI} (see Fig. 5). So, the difference in the results of the responses exists between the sink-in and the pile-up in spherical indentation as indicated by the authors[23] and as was also noted by the author[24,25] who expressed the mechanical responses as a function of the mode of

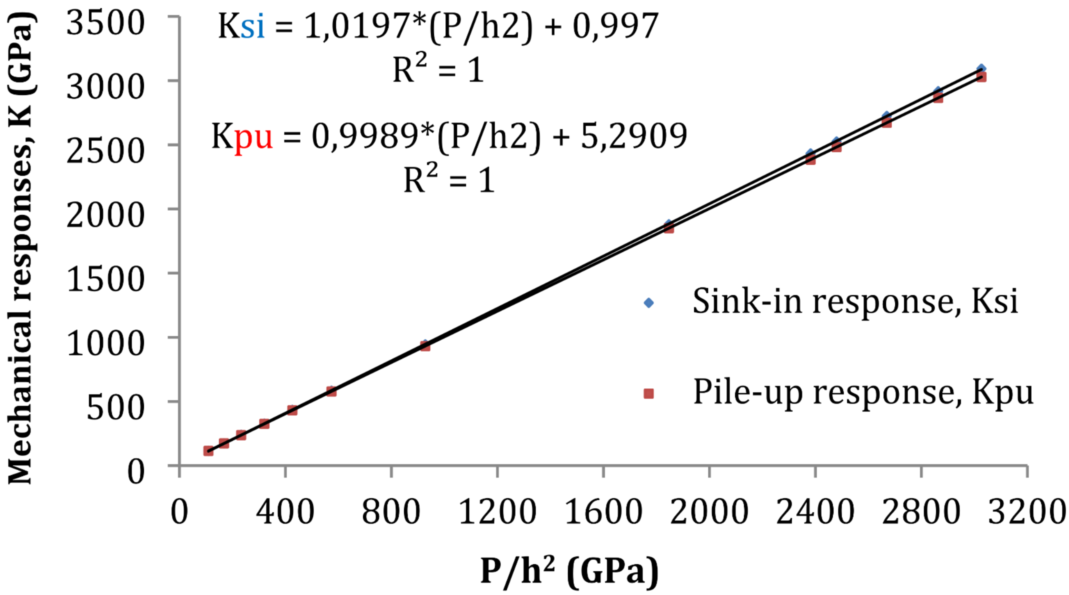

Fig. 3. Linear regressions of the two mechanical responses of the P/h^2 function by spherical indentation.

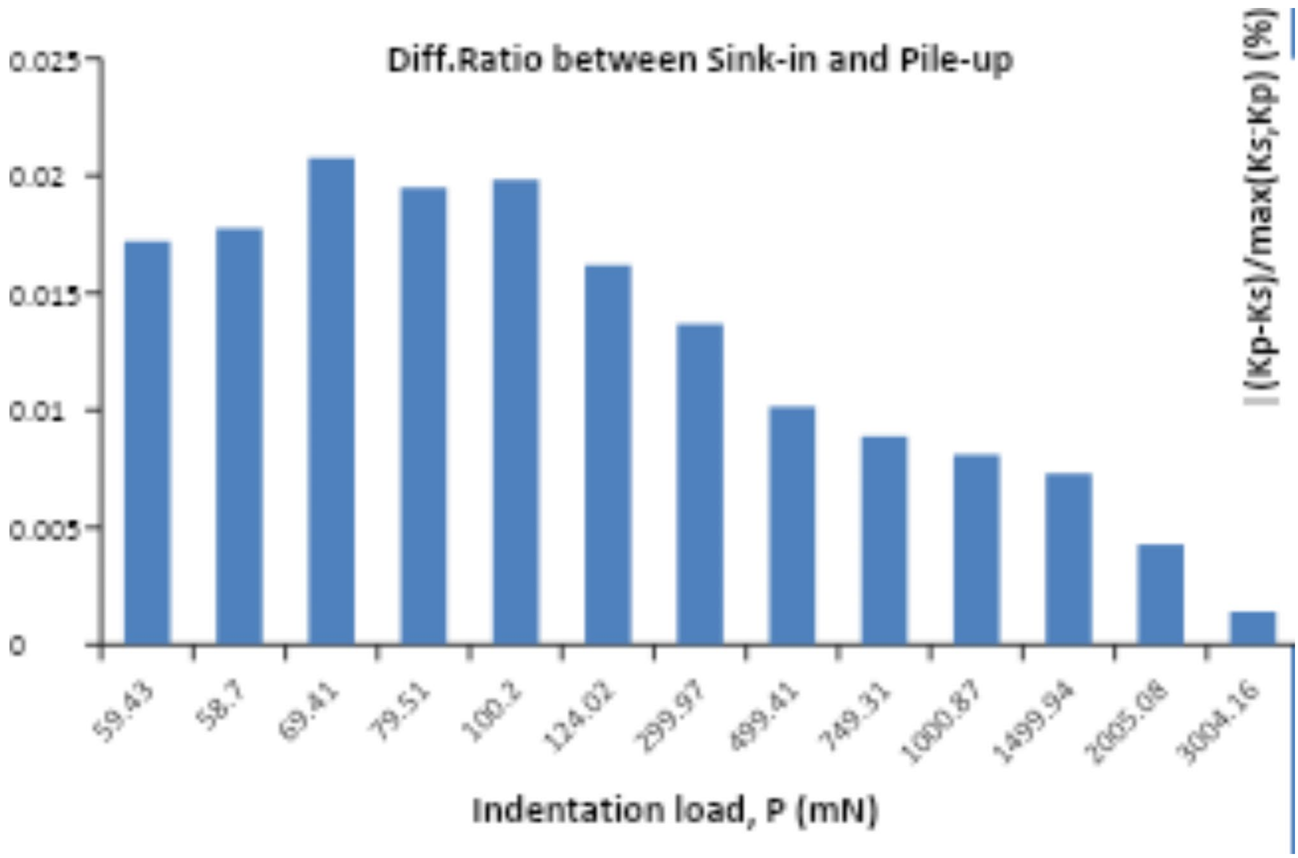

Fig. 4. Indication of the difference amplitudes between the two responses K_{SI} and K_{PU} for each indentation test.

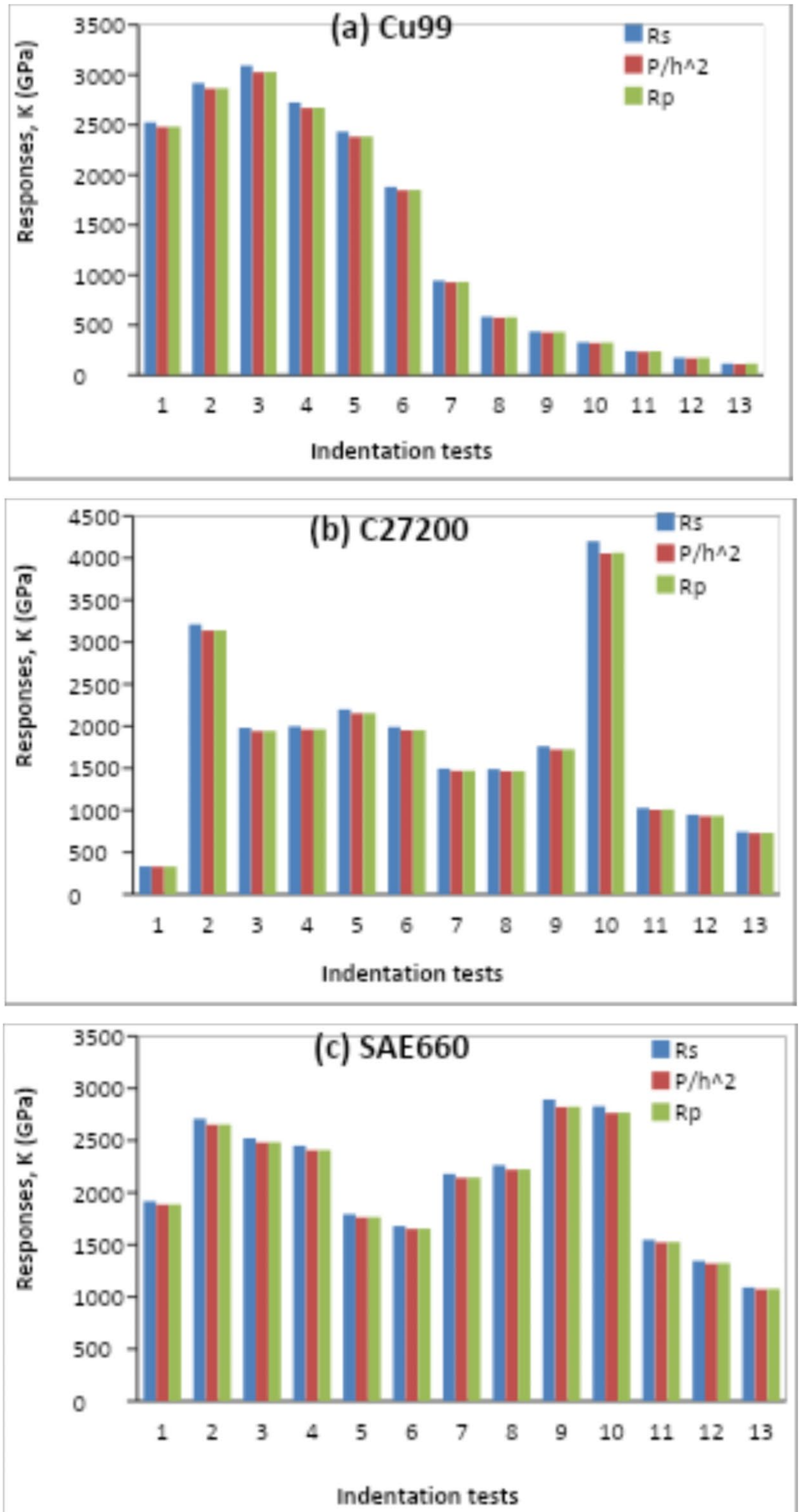

Fig. 5. Histogram of correlation between the analytical expressions relating to the sink-in[12], the pile-up (proposal of this work), and the direct (experimental) expression P/h^2 for 13 tests of spherical indentation of materials: (**a**) Cu99, (**b**) C27200, (**c**) SAE660.

	Sinking-in mode		Pile-up type	
Designation	K-exp (GPa)	$K_{SI}(GPa)$ Eq. (2)	$K_{PU}(GPa)$ Eq. (19)	Indenter geometry
SAE660	389.98	400.77	398.38	Spherical indenter
Cu99	470.40	481.10	475.35	
C27200	319.35	327.89	323.51	

Table 4. $K-$ factor considered as of the device stiffness and Young's modulus collected in Table 3 by smearing Eq. (2) as well as Eq. (19) for Fischer-Cripps[12] and present work, respectively The investigational $K-$factor is designed via all load-depth curves.

deformation under the indenter. Hence, the need to use the corresponding expression, Eq. (2) [12] or Eq. (18) according to the deformation mode determined beforehand by the h_f/h_m criterion[21,22] to correct any errors induced by ignorance of the designated mode.

Conclusions

The recommended model for this paper is specifically for spherical penetrators as it has already been refined in the case of pyramidal penetrators[11]. The empirical outcomes for the situation of the sink-in deformation mode is appropriately obtained by implementing the model from Fischer-Cripps[12]. However, the recommended model in this paper is appropriate for pile-up distortion mode, where the applied load is represented as a penetration depth with the $K-$ factor for copper and its two alloys. A difference was observed between the two mechanical responses K_{SI} and K_{PU} is estimated in percentages at 2.7%, 2.2% and 2.6% for the materials: SAE660, Cu99 and C27200, respectively. This difference constitutes the margin of error between the two modes in the case where one mode is substituted by the second by ignorance. In viewpoint, the projected ideal will be scanned in the passageway from the micro-scale to the nanometric scale by examining other expressions derived from the latter and appreciating their conditions of application.

Data availability

All data generated or analysed during this study are included in this published article.

Received: 5 September 2024; Accepted: 21 November 2024
Published online: 25 November 2024

References

1. Tabor, D. A simple theory of static and dynamic hardness. *Proc. R. Soc. A* **192**(1029), 247 (1948).
2. Stillwell, N. A. & Tabor, D. Elastic recovery of conical indentations. *Proc. Phys. Soc. London* **78**(2), 169 (1961).
3. Norbury, A. L. & Samuel, T. The recovery and sinking-in or piling-up of material in the Brinell test and the effects of these factors on the correlation of the Brinell with certain other hardness tests. *J. Iron Steel Inst.* **117**, 673–687 (1928).
4. Matthews, J. R. Indentation hardness and hot pressing. *Acta Metall.* **28**, 311–318 (1980).
5. Alcalá, J., Barone, A. C. & Anglada, M. The influence of plastic hardening on surface deformation modes around Vickers and spherical indents. *Acta Mater.* **48**, 3451–3464 (2000).
6. Taljat, B. & Pharr, G. M. Development of pile-up during spherical indentation of elastic-plastic solids. *Int. J. Sol. Struct.* **41**(3891–3904), 78910 (2004).
7. Giannakopoulos, A. E. & Zisis, Th. Analysis of Knoop indentation. *Int. J. Solids Struct.* **48**(1), 175–190 (2011).
8. Zisis, Th. & Giannakopoulos, A. E. Analysis of Knoop indentation strain hardening effects. *Int. J. Solids Struct.* **48**, 3217–3231 (2011).
9. Giannakopoulos, A. E. & Zisis, T. Analysis of Knoop indentation of cohesive frictional materials. *Mech. Mater.* **1**(57), 53–74 (2013).
10. Mesarovic, S. D. & Fleck, N. A. Spherical indentation of elastic–plastic solids. *Proceedings of the Royal Society of London. Series A: Mathematical, Physical and Engineering Sciences* **455**(1987), 2707–2728 (1999).
11. Hainsworth, S.-V., Chandler, H.-W. & Page, T.-F. Analysis of nanoindentation load-displacement loading curves. *J. Mater. Res.* **11**, 8 (1996).
12. Fischer-Cripps, A.-C. Simulation of sub-micron indentation tests with spherical and Berkovich indenters. *J. Mater. Res.* **16**(7), 2148–2157 (2001).
13. Habibi, S. et al. The P–h^2 relationship on load–displacement curve considering pile-up deformation mode in instrumented indentation. *J. Mater. Res.* **36**, 3074–3085 (2021).
14. Oliver, W.-C. & Pharr, G.-M. An improved technique for determining hardness and elastic modulus using load and displacement sensing indentation experiments. *J. Mater. Res.* **7**(6), 1564–1583 (1992).
15. Loubet, J.-L., Bauer, M., Tonck, Bec, S., and Gauthier-Manuel, B.: Nanoindentation with a surface force apparatus, Mechanical properties, and deformation behaviour of materials having ultra-fine microstructures. Kluwer Academic Publishers. 429–447 (1993).
16. Field, J.-E. and Telling, R.-H.: The Young modulus and Poisson ratio of diamond, Research Note; Cambridge, Cavendish Laboratory (1999).
17. Quinn, G.-D., Patel, P.-L. & Lloyd, I. Effect of loading rate upon conventional ceramic microindentation hardness. *J. Res. Natl. Inst. Stand. Technol.* **107**, 299–306 (2002).
18. Guillonneau, G.: Nouvelles techniques de nanoindentation pour des conditions expérimentales difficiles : très faibles enfoncements, surfaces rugueuses, température. Autre. Ecole Centrale de Lyon (2012).
19. Bec, S., Tonck, A., Georges, J.-M., Georges, E. & Loubet, J.-L. Improvements in the indentation method with a surface force apparatus. *Philos. Mag. A* **74**, 1061 (1996).
20. Hochstetter, G., Jimenez, A. & Loubet, J.-L. Strain-rate effects on hardness of glassy polymers in the nanoscale range. Comparison between quasi-static and continuous stiffness measurements. *J. Macromol. Sci. Part B.* **38**, 681–692 (1999).
21. Oliver, W.-C. & Phar, G.-M. Measurement of harness and elastic modulus by instrumented indentation: advanced in understanding and refinements to methodology. *J. Mat. Res.* **19**(1), 3–20 (2004).

22. Yetna N'Jock, M. et al. A criterion to identify sinking-in and piling-up in indentation of materials. *Int. J. Mech. Sci.* **90**, 145–150 (2015).
23. Bartier, O., Hernot, X. & Mauvoisin, G. Theoretical and experimental analysis of contact radius for spherical indentation. *Mech. Mater.* **42**, 640–656 (2010).
24. Habibi, S. The P-h^2 relationship as a function of (hf/hm) in indentation. *Frattura ed Integrità Strutturale* **62**, 613–623 (2022).
25. Semsoum, D.-E., Habibi, S., Benaissa, S. & Merzouk, H. The proposition of analytical expression HM–(√P/S) in microindentation pile-up deformation mode. *Frattura ed Integrità Strutturale* **60**, 407–415 (2022).

Acknowledgements
The authors extend their appreciation to the Deanship of Research and Graduate Studies at King Khalid University for funding this work through Large Research Project under grant number RGP2/334/45.

Author contributions
HS and FR formulated the problem. KB and SB solved the problem. HA, FR, KB, SB SSPMI, AAE and NA computed and scrutinized the results. All the authors equally contributed in writing and proof reading of the paper. All authors reviewed the manuscript.

Declarations

Competing interests
The authors declare no competing interests.

Additional information
Correspondence and requests for materials should be addressed to S.B.

Reprints and permissions information is available at www.nature.com/reprints.

Publisher's note Springer Nature remains neutral with regard to jurisdictional claims in published maps and institutional affiliations.